Available online at www.sciencedirect.com
SCIENCE DIRECT®
Cement & Concrete Composites 28 (2006) 276–292
Cement & Concrete Composites
www.elsevier.com/locate/cemconcomp

Near surface mounted CFRP laminates for shear strengthening of concrete beams

J.A.O. Barros *, S.J.E. Dias

Department of Civil Engineering, School of Engineering, University of Minho, Azurém, 4810-058 Guimarães, Portugal

Received 21 January 2005; accepted 18 November 2005
Available online 18 January 2006

Abstract

A Near Surface Mounted (NSM) strengthening technique was developed to increase the shear resistance of concrete beams. The NSM technique is based on fixing, by epoxy adhesive, Carbon Fiber Reinforced Polymer (CFRP) laminates into pre-cut slits opened in the concrete cover of lateral surfaces of the beams. To assess the efficacy of this technique, an experimental program of four-point bending tests was carried out with reinforced concrete beams failing in shear. Each of the four tested series was composed of five beams: without any shear reinforcement; reinforced with steel stirrups; strengthened with strips of wet lay-up CFRP sheets, applied according to the externally bonded reinforcement (EBR) technique; and two beams strengthened with NSM precured laminates of CFRP, one of them with laminates positioned at 90° and the other with laminates positioned at 45° in relation to the beam axis. Influences of the laminate inclination, beam depth and longitudinal tensile steel reinforcement ratio on the efficacy of the strengthening techniques were analyzed. Amongst the CFRP strengthening techniques, the NSM with laminates at 45° was the most effective, not only in terms of increasing beam shear resistance but also in assuring larger deformation capacity at beam failure. The NSM was also faster and easier to apply than the EBR technique. The performance of the *ACI* and *fib* analytical formulations for the EBR shear strengthening was appraised. In general, the contribution of the CFRP systems predicted by the analytical formulations was slightly larger than the values registered experimentally. Performance of the formulation by Nanni et al. for NSM strengthening technique was also appraised. Using bond stress and CFRP effective strain values obtained in pullout bending tests with NSM CFRP laminate system, the formulation by Nanni et al. predicted a contribution of this CFRP system for the beam shear resistance of 72% the experimentally recorded values.

Keywords: Carbon fiber reinforced polymers; Concrete; Steel stirrups; Shear strengthening; Shear failure; Near surface mounted (NSM)

1. Introduction

To increase the shear resistance of concrete beams, sheets and laminates of carbon fiber reinforced polymers (CFRP) are generally applied on the faces of the elements to be strengthened, using an externally bonded reinforcing (EBR) technique. Adopting the EBR technique, several researchers have verified that the shear resistance of concrete beams can significantly be increased [1–6]. However, due to premature debonding of the FRP, the maximum strain mobilized by these systems is well below their ultimate strain.

In an attempt to overcome this drawback, a promising strengthening innovation has been proposed by De Lorenzis [7]. Using rods of CFRP embedded into grooves on the concrete cover of lateral faces of the beams, a significant increase on beam load carrying capacity was obtained. Assuring the proper bond conditions for the rod into the groove is the critical phase of this strengthening technique, since it requires special equipment, well-prepared technical staff and a significant time consuming execution period. In the experimental program carried out by De Lorenzis and Nanni [8] for the characterization of the bond properties of NSM FRP rods, the grooves were created by saw-cutting

* Corresponding author. Tel.: +351 253 510 210; fax: +351 253 510 217.
E-mail address: barros@civil.uminho.pt (J.A.O. Barros).

0958-9465/$ - see front matter © 2005 Elsevier Ltd. All rights reserved.
doi:10.1016/j.cemconcomp.2005.11.003

two parallel slits at the desired distance and depth, and chiseling off the material in between, which is a too time consuming procedure for real applications. In another experimental program [9], the grooves were pre-formed rather than cut after concrete hardening. This procedure only replicates the real conditions if the concrete cover of the element to be strengthened is deteriorated and needs to be replaced. In such a case, pre-form the grooves while reconstructing the element geometry might be a correct strategy.

In the present work, a technique similar to the previous one was used for the shear strengthening of concrete beams with the difference that, instead of rods, laminates were used. Since the laminates had a cross section of about $1.4 \times 10\ mm^2$, they were installed into thin slits, which were easily cut using conventional saw-cut equipment. Furthermore, a high uniformity on the cross section dimensions of the slits can be assured, with the derived benefits in terms of homogeneity in CFRP–concrete bond properties. This strengthening technique has already proven to be very effective for the flexural strengthening of reinforced concrete columns [10] and beams [11]. The bond behavior was also well characterized by pullout bending tests [12] and a local bond stress-slip relationship was evaluated [13], which can be used in the analysis and design of concrete elements strengthened by this technique.

To evaluate the efficacy of the shear strengthening technique proposed in the present work, the behavior of beams strengthened according to this technique was compared to the behavior of beams reinforced with conventional steel stirrups and with the behavior of beams strengthened by strips of wet lay-up CFRP sheet. The experimental program was designed to analyze the influences of beam depth, NSM laminate inclination, and longitudinal tensile steel reinforcement ratio on the shear strengthening. In the present work, the tests carried out are described and the main results are presented and analyzed.

The performance of the *ACI* [14] and *fib* [15] analytical formulations for the EBR shear strengthening was appraised. Additionally, the performance of the analytical formulation proposed by Nanni et al. [16] is assessed.

2. Experimental program

2.1. Test series

The experimental program is composed of four test series (Table 1 and Fig. 1). Each series is made up of a beam without any shear reinforcement (C) and a beam for each of the following shear reinforcing systems: steel stirrups of ϕ6 mm (S), U shaped strips of CFRP sheet (M) and CFRP laminates at 45° (IL) or at 90° (VL) with the beam axis. Series A10 and A12 are composed of beams with a cross section of $0.15 \times 0.30\ m^2$ and a span length of 1.5 m. Series B10 and B12 are constituted of beams with a cross section of $0.15 \times 0.15\ m^2$ and a span length of 0.9 m. To evaluate the influence of the longitudinal tensile steel reinforcement ratio, ρ_{sl}, series A10 and B10 had 4ϕ10 steel bars at beam bottom tensile surface, while A12 and B12 series had 4ϕ12. The shear span, a, (Fig. 1) in both series of beams, was twice the depth of the corresponding beams. At top surface, the beams of all series were reinforced with 2ϕ6 steel bars. The concrete clear cover for the top, bottom and lateral faces of the beams was 15 mm.

The amount of shear reinforcement applied in the four reinforcing systems was designed such that all beams would

Table 1
Series of tests

Beam designation			Shear strengthening systems			
			Material	Quantity	Spacing (mm)	Angle (°)
A series	A10 series	A10_C	–	–	–	–
		A10_S	Steel stirrups	6ϕ6 of two branches	300	90
		A10_M	Strips of S&P C-Sheet 530	8 × 2 layers of 25 mm (U shape)	190	90
		A10_VL	S&P laminates of CFK 150/2000	16 CFRP laminates	200	90
		A10_IL	S&P laminates of CFK 150/2000	12 CFRP laminates	300	45
	A12 series	A12_C	–	–	–	–
		A12_S	Steel stirrups	10ϕ6 of two branches	150	90
		A12_M	Strips of S&P C-Sheet 530	14 × 2 layers of 25 mm (U shape)	95	90
		A12_VL	S&P laminates of CFK 150/2000	28 CFRP laminates	100	90
		A12_IL	S&P laminates of CFK 150/2000	24 CFRP laminates	150	45
B series	B10 series	B10_C	–	–	–	–
		B10_S	Steel stirrups	6ϕ6 of two branches	150	90
		B10_M	Strips of S&P C-Sheet 530	10 × 2 layers of 25 mm (U shape)	80	90
		B10_VL	S&P laminates of CFK 150/2000	16 CFRP laminates	100	90
		B10_IL	S&P laminates of CFK 150/2000	12 CFRP laminates	150	45
	B12 series	B12_C	–	–	–	–
		B12_S	Steel stirrups	10ϕ6 of two branches	75	90
		B12_M	Strips of S&P C-Sheet 530	16 × 2 layers of 25 mm (U shape)	40	90
		B12_VL	S&P laminates of CFK 150/2000	28 CFRP laminates	50	90
		B12_IL	S&P laminates of CFK 150/2000	24 CFRP laminates	75	45

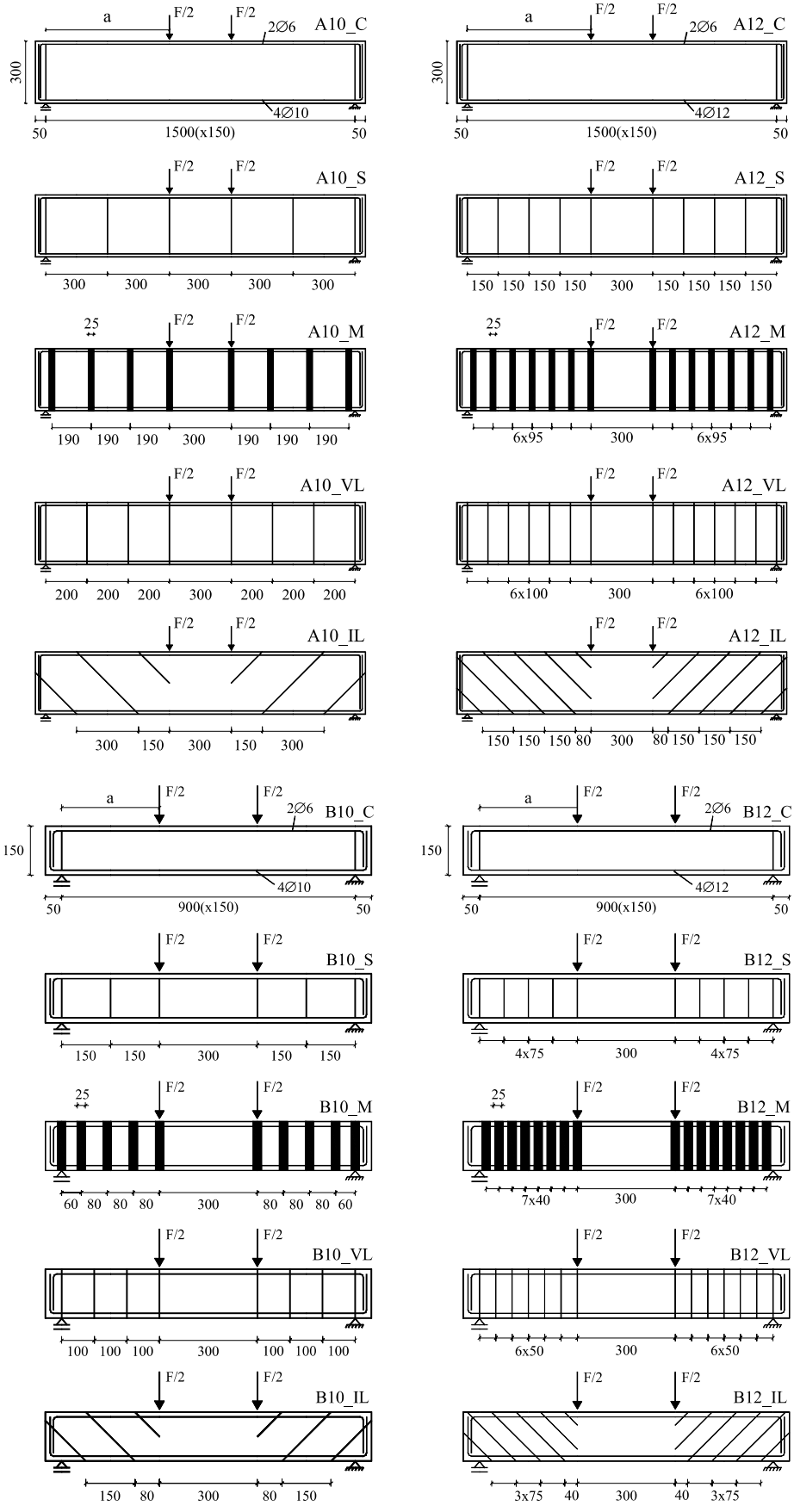

Fig. 1. Beam series.

fail in shear, at a similar maximum load. For this purpose, the strategy adopted for the evaluation of the distinct shear reinforcing systems was the following. The beam flexural load carrying capacity, $F_{\text{rupture}}^{\text{flexural}}$, for each ρ_{sl} was evaluated. The concrete contribution for the beam shear resistance was determined according to the Portuguese Code, that is similar to the CEB-FIP Model Code [17] but the dowel effect is not considered ($V_{\text{cd}}^{\text{ana}} = \tau_1 b_{\text{w}} d$, where τ_1 is the concrete shear strength and b_{w} and d are the beam width and the effective depth, respectively). The percentage of steel stirrups was evaluated according to Portuguese Code ($V_{\text{wd}}^{\text{ana}} = 0.9d\frac{A_{\text{sw}}}{s}f_{\text{syd}}$, where s, f_{syd} and A_{sw} are the spacing, the design yield stress and the cross section area of the two arms steel stirrups, respectively). This percentage was determined in order to provide a beam shear load carrying capacity ($2V_{\text{cd}}^{\text{ana}} + 2V_{\text{wd}}^{\text{ana}}$) lesser than $F_{\text{rupture}}^{\text{flexural}}$. According to the arrangements of the steel stirrups adopted in the beam series (Fig. 1), the $F_{\text{rupture}}^{\text{flexural}}/(2V_{\text{cd}}^{\text{ana}} + 2V_{\text{wd}}^{\text{ana}})$ ratio was 1.05, 1.08, 1.5 and 1.37 for the A10, A12, B10 and B12 series.

The percentage of the CFRP shear reinforcing systems was evaluated to provide a contribution for the beam shear resistance similar to that of the steel stirrups. For the strips of wet lay-up CFRP sheets of U shape, the recommendations of the ACI Committee 440 were followed [14]. For the NSM CFRP laminates, the formulation used for the steel stirrups was adopted. The yield stress was, however, replaced by an effective stress that was determined assuming a CFRP strain value of 4‰, which is the maximum effective strain value recommended by ACI Committee 440 for the EBR shear reinforcing systems.

Steel stirrups were not applied in the series reinforced with CFRP systems. The interaction between the CFRP shear reinforcement and the steel stirrups will be only investigated in future experimental programs.

2.2. Material properties

2.2.1. Concrete and steel bars

The average compressive strength (f_{cm}) at 28 days and at the date of beam testing was evaluated from uniaxial compression tests with cylinders of 150 mm diameter and 300 mm height. At 28 days, series A and B had a f_{cm} of 37.6 and 49.5 MPa, respectively. At beam testing age of 227 and 105 days for series A and B, respectively, the f_{cm} of series A and B was 49.2 and 56.2 MPa. The properties of the steel bars were obtained from uniaxial tensile tests, carried out according to European standard EN 10 002-1 [18]. The registered results are included in Table 2.

2.2.2. CFRP systems

Unidirectional wet lay-up sheets of a trademark S&P C-Sheet 530 and precured laminates of a trademark S&P laminate CFK 150/2000 were the two CFRP systems used in the present work. According to the supplier, tensile strength (f_{fu}^*), Young's modulus (E_{f}) and ultimate strain ($\varepsilon_{\text{fu}}^*$) of the sheets and laminates have the following values: $f_{\text{fu}}^* = 3000$ MPa, $E_{\text{f}} = 390{,}000$ MPa and $\varepsilon_{\text{fu}}^* = 0.8\%$ for sheets; and $f_{\text{fu}}^* = 2200$ MPa, $E_{\text{f}} = 150{,}000$ MPa and $\varepsilon_{\text{fu}}^* = 1.4\%$ for laminates. The sheet had a thickness of 0.167 mm, while the cross section of the laminate had a width of 10 mm and a thickness of 1.4 mm. For the laminates, six tests were also carried out according to the ISO 527-5 recommendations [19], from which the following average values were obtained: $f_{\text{fu}} = 2286$ MPa, $E_{\text{f}} = 166{,}000$ MPa and $\varepsilon_{\text{fu}} = 1.3\%$.

Table 2
Properties of steel bars

Series	Stress	ϕ6 (long.)	ϕ6 (trans.)	ϕ10 (long.)	ϕ12 (long.)
A	f_{sym}[a] (MPa)	622	540	464	574
	f_{sum}[b] (MPa)	702	694	581	672
B	f_{sym}[a] (MPa)	618	540	464	571
	f_{sum}[b] (MPa)	691	694	581	673

[a] Average value of the yield stress.
[b] Average value of the maximum stress.

2.3. Strengthening techniques

The EBR and NSM strengthening techniques are represented in Fig. 2. To apply the wet lay-up CFRP strengthening system, the following procedures were done: (1) on the zones of the beam's surfaces where the strips of CFRP sheet would be glued, an emery was applied to remove the superficial cement paste and to round out the beam edges; (2) the residues were removed by compressed air; (3) a layer of primer was applied to regularize the concrete surface and to enhance the adherence capacity of the concrete substrate; and (4) strips of U shape CFRP sheet, composed of two layers, were glued to the bottom and to the lateral faces of the beam, by epoxy resin.

To apply the precured laminates, the following procedures were mobilized: (1) slits of about 5 mm width and 12 mm depth were made, in previously marked places, on both lateral surfaces of the beam; (2) the slits were cleaned by compressed air; (3) the laminates were cleaned by acetone; (4) the slits were filled with epoxy adhesive manufactured according to the supplier recommendations; (5) a thin layer of epoxy adhesive was applied on the faces of the CFRP laminates; and (6) the CFRP laminates were introduced into the slits after which the excess epoxy adhesive was removed.

2.4. Test set-up

The beams were subjected to four point loads (Fig. 1). The force was measured from a load cell of 300 kN maximum capacity and 0.06% linearity. To evaluate the beam deflection, five LVDTs of 25 mm and 50 mm full stroke were used, placed at mid span, under point loads and at middle of the shear span. To avoid the register of extraneous deflections (concrete crushing at beam supports, deformability of the reaction frame, etc.), the LVDTs were supported on a "Japanese Yoke" system [20–22]. The tests

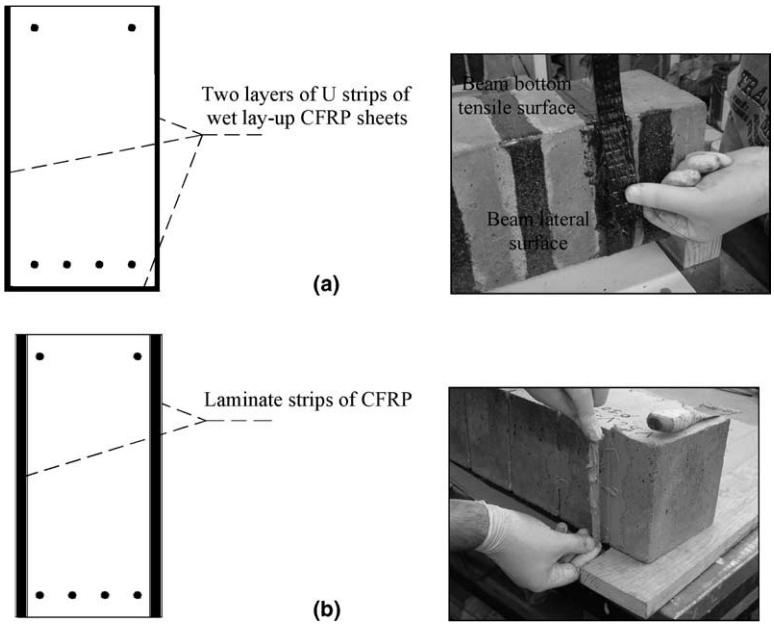

Fig. 2. Strengthening techniques: (a) external bonded, (b) near surface mounted.

were carried out under displacement control, using a deflection rate of 10 μm/s imposed on the LVDT placed at the beam mid span.

3. Results

Defining F_{max,K_C} and F_{max,K_S} as the maximum load of a beam without shear reinforcement and a beam reinforced with steel stirrups, respectively, (K represents the series of tests) the ratios $F_{max,K}/F_{max,K\_C}$ and $F_{max,K}/F_{max,K\_S}$ were determined to assess the efficacy of the shear strengthening techniques, in terms of the increase of the beam load carrying capacity. To define the deformation capacity and the retention of the load carrying capacity in the structural softening phase of the beams, provided by each shear strengthening technique, a deflection, $\delta_{p,K}$, corresponding to $0.95F_{max,K}$ beyond the deflection at the peak load, $\delta_{Fmax,K}$, was determined (Fig. 3). This deflection level was selected since it represents the beam deformation capacity for a reduced loss of the beam load carrying capacity (only 5%) in the structural softening phase. The deformation capacity was evaluated from the ratios $\delta_{p,K}/\delta_{p,K\_C}$ and $\delta_{p,K}/\delta_{p,K\_S}$ (termed the deformability indices) where δ_{p,K_C} and δ_{p,K_S} are the deflections for $0.95F_{max,K\_C}$ and $0.95F_{max,K\_S}$, respectively.

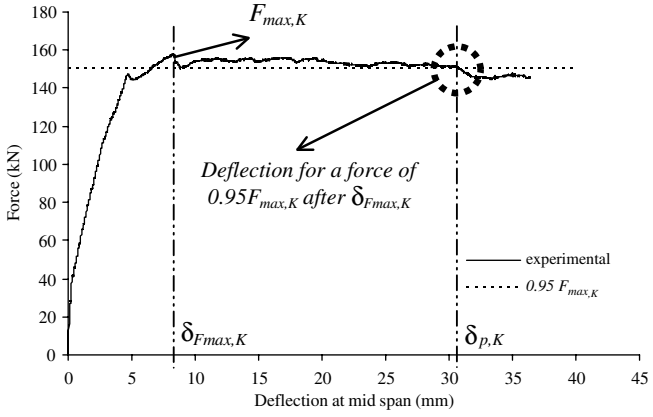

Fig. 3. Concept of $\delta_{p,K}$: deflection at $0.95F_{max,K}$ after $\delta_{Fmax,K}$.

3.1. A10 series

For the A10 series, the relationship between the force and the deflection at beam mid span is depicted in Fig. 4. Table 3 includes the main results obtained in this series. When compared to the maximum force of the unreinforced beam (A10_C), Fig. 4 and Table 3 show that the CFRP shear strengthening systems increased the maximum load between 22% (A10_M) and 58% (A10_VL and A10_IL). The F_{max} of the A10_M, A10_VL and A10_IL beams (strengthened with CFRP systems) was 28%, 6% and 7% less than the F_{max} of the beam reinforced with steel stirrups (A10_S). The highest deformation capacity was registered in the beam strengthened with inclined laminates (A10_IL). In comparison with $\delta_{p,A10\_C}$ (unreinforced beam), the $\delta_{p,A10\_S}$, $\delta_{p,A10\_M}$, $\delta_{p,A10\_VL}$ and $\delta_{p,A10\_IL}$ were 480%, 34%, 359% and 1006% larger. When compared to the beam reinforced with steel stirrups (A10_S), the deformation capacity of the A10_IL beam was 91% higher.

3.2. A12 series

Fig. 5 depicts, for the A12 series, the relationship between the force and the deflection at beam mid span. Table 3 includes the main results obtained in this series. Taking the F_{max} of A12_C beam as a reference value, the

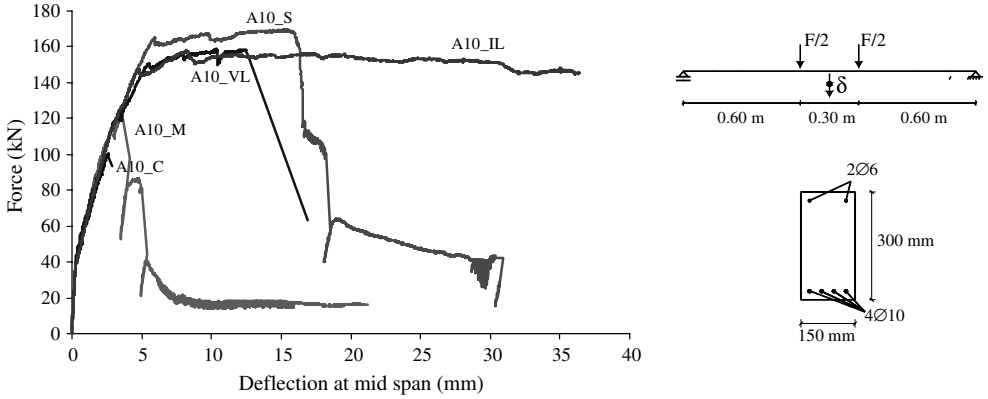

Fig. 4. Force vs deflection relations of the A10 beam series.

Table 3
Main results

Beam designation	Shear reinforcing system	$F_{max,K}$ (kN)	$\frac{F_{max,K}}{F_{max,K\_C}}$	$\frac{F_{max,K}}{F_{max,K\_S}}$	$\delta_{p,K}$ (mm)	$\frac{\delta_{p,K}}{\delta_{p,K\_C}}$	$\frac{\delta_{p,K}}{\delta_{p,K\_S}}$
A10_C	–	100.40	1.00	0.59	2.80	1.00	0.17
A10_S	Steel stirrups	169.35	1.69	1.00	16.25	5.80	1.00
A10_M	Strips of sheet	122.06	1.22	0.72	3.75	1.34	0.23
A10_VL	Vertical laminates	158.64	1.58	0.94	12.86	4.59	0.79
A10_IL	Inclined laminates	157.90	1.57	0.93	30.96	11.06	1.91
A12_C	–	116.50	1.00	0.54	2.74	1.00	0.43
A12_S	Steel stirrups	215.04	1.85	1.00	6.34	2.31	1.00
A12_M	Strips of sheet	179.54	1.54	0.83	4.91	1.79	0.77
A12_VL	Vertical laminates	235.11	2.02	1.09	6.70	2.45	1.06
A12_IL	Inclined laminates	262.38	2.25	1.22	11.75	4.29	1.85
B10_C	–	74.02	1.00	0.61	2.00	1.00	0.23
B10_S	Steel stirrups	120.64	1.63	1.00	8.53	4.27	1.00
B10_M	Strips of sheet	111.14	1.50	0.92	4.40	2.20	0.52
B10_VL	Vertical laminates	131.22	1.77	1.09	6.83	3.42	0.80
B10_IL	Inclined laminates	120.44	1.63	1.00	4.27	2.14	0.50
B12_C	–	75.70	1.00	0.48	2.03	1.00	0.40
B12_S	Steel stirrups	159.10	2.10	1.00	5.09	2.51	1.00
B12_M	Strips of sheet	143.00	1.89	0.90	3.52	1.73	0.69
B12_VL	Vertical laminates	139.20	1.84	0.87	4.44	2.19	0.87
B12_IL	Inclined laminates	148.50	1.96	0.93	4.92	2.42	0.97

steel stirrups provided an 85% increase in F_{max}, while CFRP strengthening systems assured an increase ranging between 54% and 125%, where the highest value was registered in the beam strengthened with inclined laminates (A12_IL), and the lowest value in the beam with strips of wet lay-up sheet (A12_M). Comparing the F_{max} of the beams strengthened by CFRP systems with the beam reinforced with steel stirrups (A12_S), the F_{max} of A12_M was 17% smaller and the F_{max} of A12_VL and A12_IL beams was 9% and 22% larger, respectively. The higher efficacy of the laminates at 45° was also notable in terms of deformation capacity. When compared with δ_p of beam A12_C ($\delta_{p,A12\_C}$), the δ_p of A12_S, A12_VL and A12_IL beams was 131%, 145% and 329% larger, respectively, i.e., the beam strengthened with inclined laminates was 85% more deformable than the beam reinforced with steel stirrups. The deformation capacity of A12_M beam was 77% of the deformation of A12_S beam.

3.3. B10 series

For the B10 series, Fig. 6 illustrates the relationship between the force and the deflection at beam mid span. The main results are included in Table 3. Taking into account the load of the beam without any shear reinforcement, $F_{max,B10\_C}$, the steel stirrups provided an increase of 63% in the F_{max}, while the increase assured by CFRP shear strengthening systems ranged between 50% and 77%, where the highest value was registered in the beam with vertical laminates (B10_VL), and the lowest value in the beam with strips of sheet (B10_M). Taking the maximum force of the beam reinforced with steel stirrups ($F_{max,B10\_S}$) as a basis of comparison, it was verified that the maximum load of B10_M, B10_VL and B10_IL beams was 92%, 109% and 100% of the $F_{max,B10\_S}$, respectively. The better performance of the vertical laminate shear reinforcing system was more pronounced in terms of beam deformation

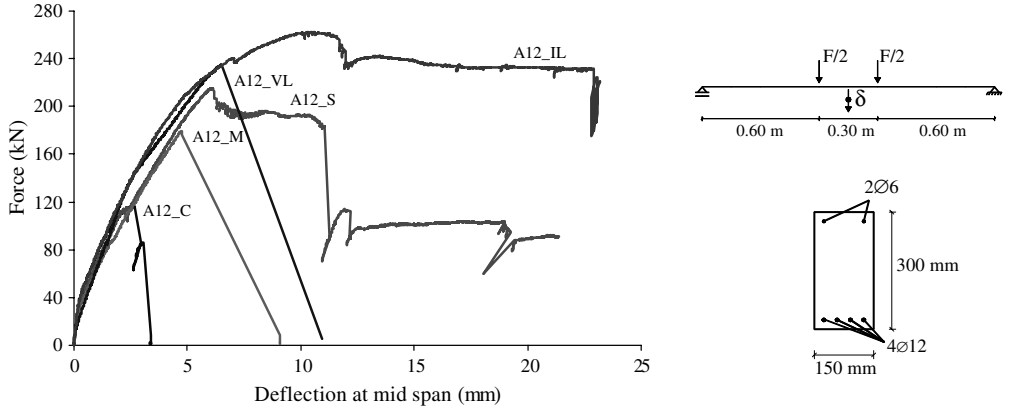

Fig. 5. Force vs deflection relations of the A12 beam series.

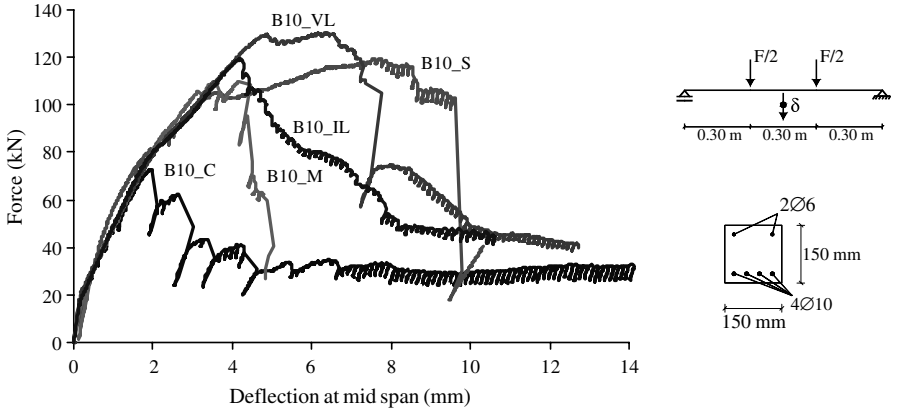

Fig. 6. Force vs deflection relations of the B10 beam series.

capacity. In fact, the beams reinforced with steel stirrups, vertical laminates, inclined laminates and strips of sheet had a δ_p 327%, 242%, 114% and 120% larger than the δ_p of the beam without any shear reinforcement. The deformation capacity of the beam reinforced with vertical laminates was 80% of that of the beam reinforced with steel stirrups.

3.4. B12 series

For the B12 series, the relationship between the force and the deflection at beam mid span is depicted in Fig. 7. The main results are included in Table 3. When compared to the maximum load of the beam without any shear reinforcement, $F_{max,B12\_C}$, it is observed that steel stirrups provided

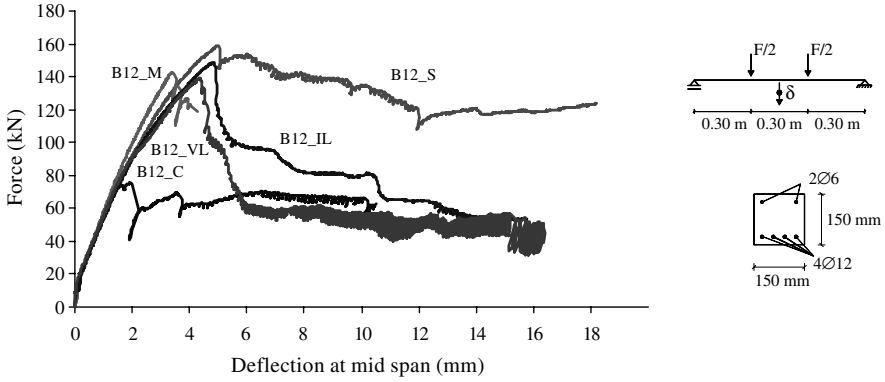

Fig. 7. Force vs deflection relations of the B12 beam series.

an increase of 110% in the F_{max}, while the increase assured by CFRP shear strengthening systems ranged from 84% to 96%, where the highest value was recorded in the beam with inclined laminates (B12_IL), and the lowest value in the beam with vertical laminates (B12_VL). Using the maximum force of the beam reinforced with steel stirrups ($F_{max,B12\_S}$) as a basis of comparison, it was verified that the maximum load of B12_M, B12_VL and B12_IL beams was 90%, 87% and 93% of the $F_{max,B12\_S}$, respectively. In terms of deformation capacity, the better CFRP strengthening system was the one composed of inclined laminates. When the δ_p of the beam without any shear reinforcement

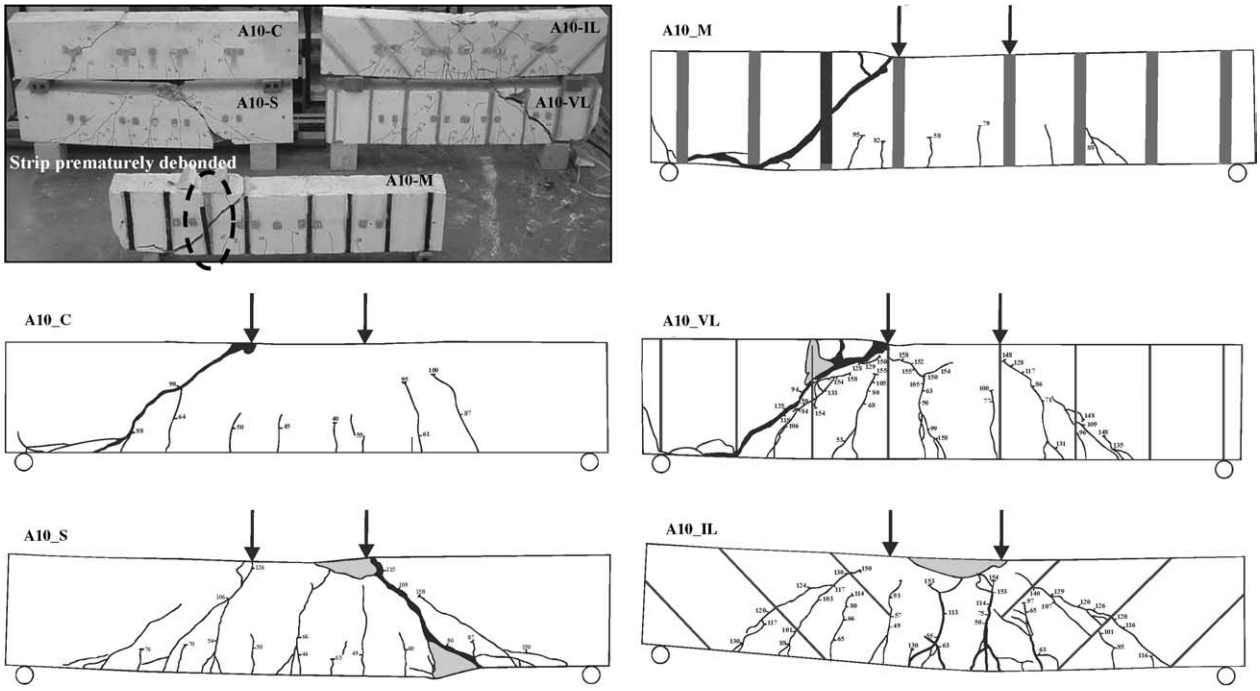

Fig. 8. Failure modes of A10 beam series.

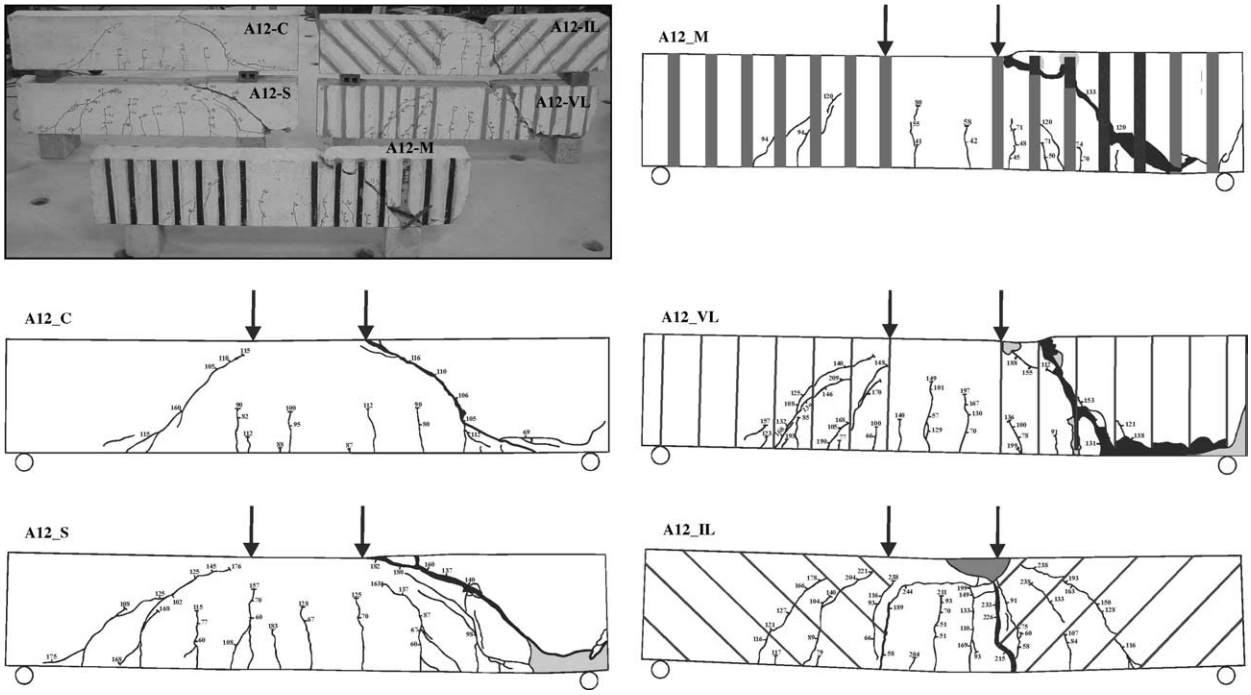

Fig. 9. Failure modes of A12 beam series.

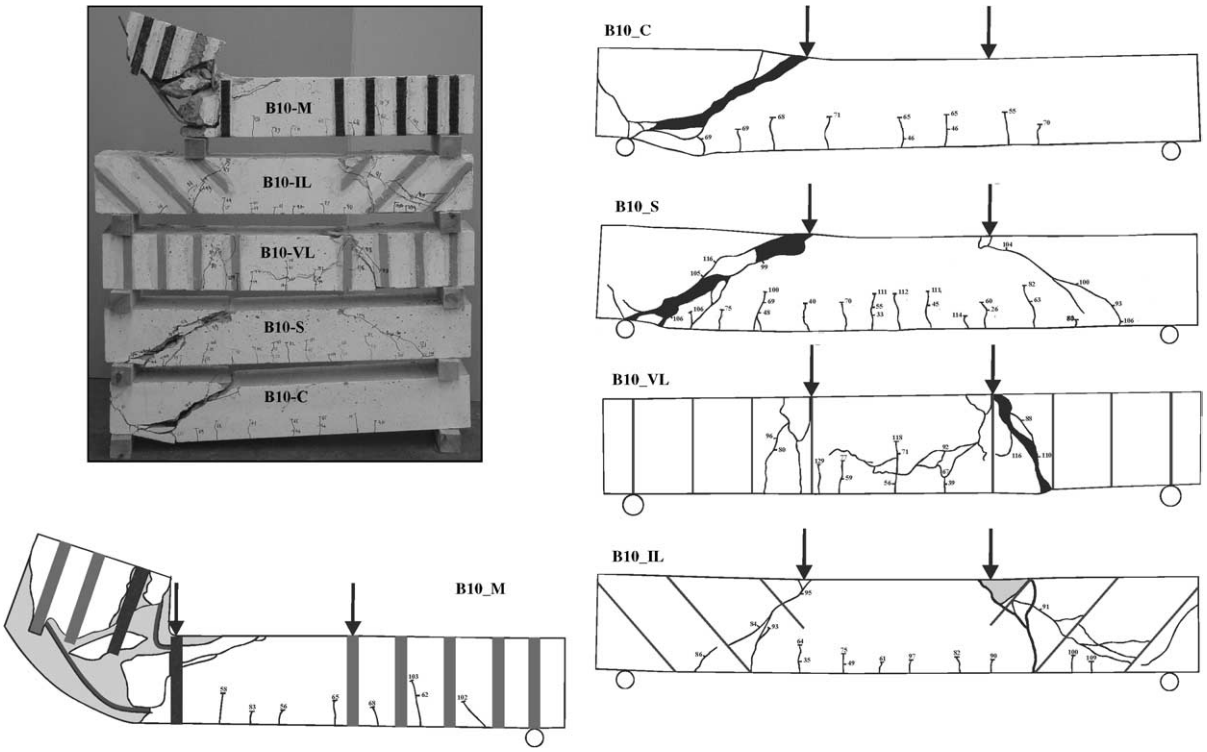

Fig. 10. Failure modes of B10 beam series.

($\delta_{p,B12\_C}$) is compared to the δ_p of the remaining beams, an increase of 151%, 73%, 119% and 142% was obtained in the B12_S, B12_M, B12_VL and B12_IL beams, respectively, showing that the deformation capacity of the beam with inclined laminates was 97% of that of the beam reinforced with steel stirrups.

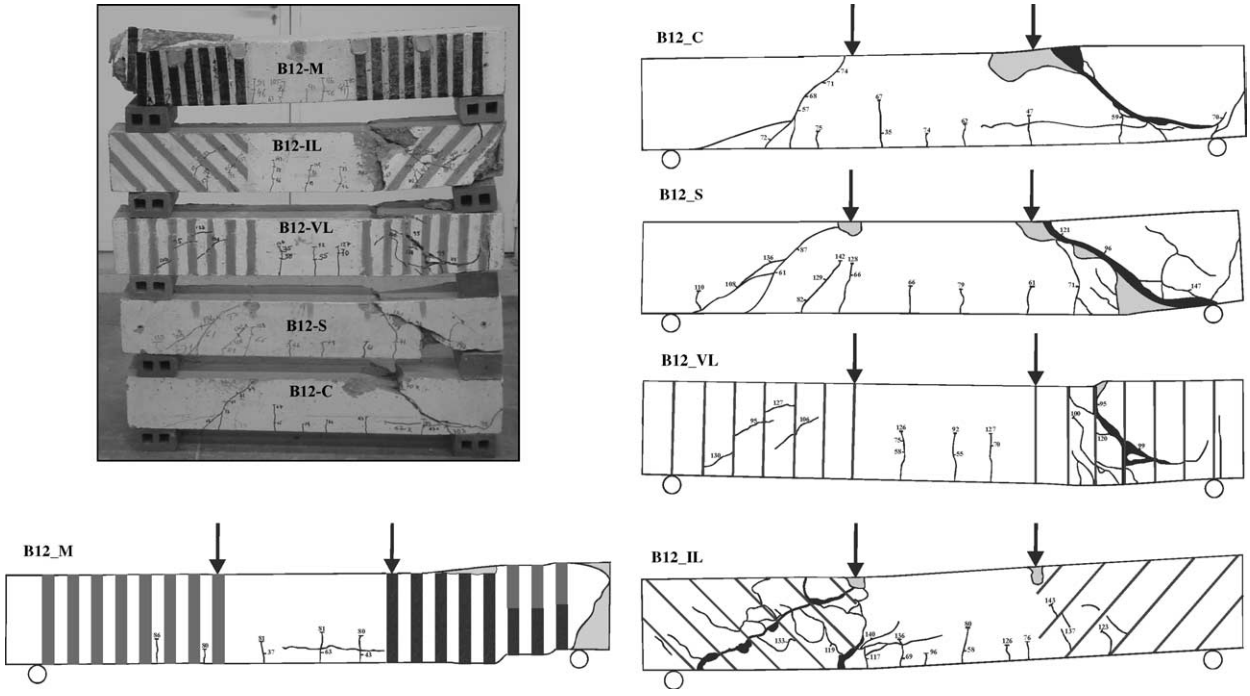

Fig. 11. Failure modes of B12 beam series.

3.5. Failure modes

Figs. 8–11 include photos of the beams after they have been tested. A representation of the failure modes is also depicted. The unreinforced shear C beams have failed by the formation of one shear failure crack without the yielding of the longitudinal tensile reinforcement. A shear failure crack occurred in the beams reinforced with steel stirrups (S beams). However, in beams A10_S (Fig. 8) and A12_S (Fig. 9) this shear failure crack occurred after the yielding of the longitudinal tensile reinforcement since the flexural load carrying capacity ($F_{\text{rupture}}^{\text{flexural}}$) of these beams is only 5–8% higher than the combined contribution of the concrete and steel stirrups ($2V_{\text{cd}}^{\text{ana}} + 2V_{\text{wd}}^{\text{ana}}$) for the beam shear resistance (see subsection "Test Series" of Section 2). Since $F_{\text{rupture}}^{\text{flexural}}$ of the beams B10_S (Fig. 10) and B12_S (Fig. 11) is 50% and 37% higher than the ($2V_{\text{cd}}^{\text{ana}} + 2V_{\text{wd}}^{\text{ana}}$) of these beams, they were failed by the formation of a shear crack before the yielding of the longitudinal tensile reinforcement.

The sudden loss of the load carrying capacity in the S beams corresponds to the moment when a steel stirrup, crossing the shear failure crack, ruptured. Due to the combined crack opening and crack sliding of the shear failure crack, a stress gradient occurred in the cross section of the steel stirrup crossing the shear failure crack, leading to its rupture. This stress gradient was significant since only one steel stirrup was crossing the shear failure crack.

In general, beams M failed by the formation of a shear crack. In Figs. 8–11, the darkest parts of the CFRP strips represent the length that peeled-off. Due to the U configuration of the CFRP strips, the peeled-off process propagated from the top to the bottom of the beam (Fig. 12a). In these beams, immediately after the CFRP strips crossing the shear failure crack have peeled-off, the CFRP strips crossing the horizontal path of the shear crack have ruptured due to an abrupt increment of tensile and shear stresses in the CFRP, as a result of the crack opening and crack sliding (Fig. 12a). B12_M beam (Fig. 12b) had a distinct failure mode. This beam failed

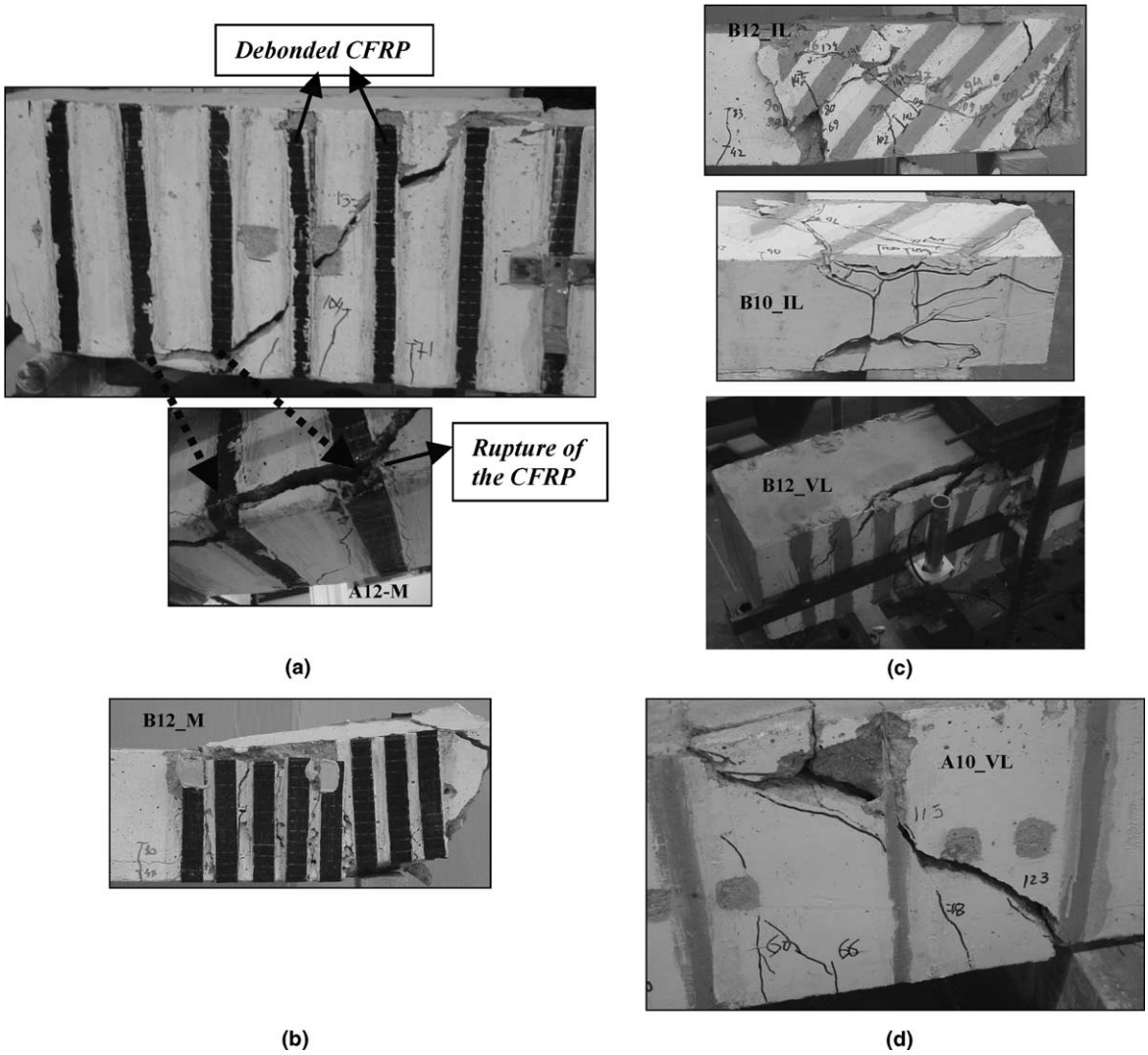

Fig. 12. Details of the failure modes: (a) A12_M, (b) B12_M, (c) B12_IL, B10_IL and B12_VL, (d) A10_VL.

by the formation of two "concrete lateral walls" that have separated from the interior concrete volume. A shear crack formed in this interior concrete volume and, finally, the "lateral walls" ruptured. The justification for this distinct failure mode can reside on the ratio between the area of the CFRP strips bonded to the beam lateral surfaces and the area of the beam lateral surfaces, since it is the highest one of the M beams. Due to the high percentage of CFRP strips in B12_M beam, the shear failure crack did not extend to the total width of the beam. Two lateral walls of 15–20 mm thick, reinforced with the strips, have spoiled, leading to a failure mode composed by the beam core, failed in shear, and two lateral reinforced walls, detached from this core.

This complex type of failure also occurred in beams B10_IL, B12_VL and B12_IL, due to similar reasons (Fig. 12c).

In A10_VL beam, after the yielding of the longitudinal tensile reinforcement, a shear failure crack formed. During the opening process of this crack, the shorter bond length of the CFRP laminate, crossing this crack, slip (Fig. 12d).

Beams A12_VL failed in shear and the shorter bond length of the CFRP laminate, crossing this crack, slip. Finally, beams A10_IL and A12_IL ruptured by the formation of a flexural failure crack.

3.6. Influence of test parameters on the efficacy of the CFRP shear strengthening systems

Fig. 13 represents the influence of the CFRP shear reinforcement ratio (ρ_f), the beam depth (h) and the longitudinal tensile steel reinforcement (ρ_{sl}) on the beam load carrying capacity provided by the considered CFRP shear reinforcing systems. The ΔF_{max} corresponds a two times the contribution of the CFRP systems for the beam shear resistance (V_f), since $\Delta F_{max} = F_{max,K} - F_{max,K\_C} = 2V_f$. To take into account the distinct values of Young's modulus of the CFRP materials, the ρ_f of the CFRP sheets was converted into an equivalent percentage of CFRP laminates, multiplying its percentage by the E_{f_M}/E_{f_L} parameter, where E_{f_M} and E_{f_L} are Young's modulus of the sheets and laminates, respectively.

From the analysis of Fig. 13a it can be concluded that ΔF_{max} increased with ρ_f and this increase was more significant in the highest beams strengthened by NSM technique. Fig. 13b shows that, for the beams strengthened by EBR technique the ΔF_{max} decreased with the increase of the beam depth, while in the beams strengthened by NSM technique the ΔF_{max} increased with the increase of the beam depth. This increase was more pronounced in the beams of high longitudinal tensile reinforcement ratio (4ϕ 12), mainly when laminates are positioned at 45°. This can be justified by the values of the total effective length of the CFRP laminates ($L_{tot\,min}$) contributing for the beam shear resistance, which concept is described in Subsection "*Formulation by Nanni et al. for NSM technique*" of Section 4, since it was verified that ΔF_{max} has an increase linear

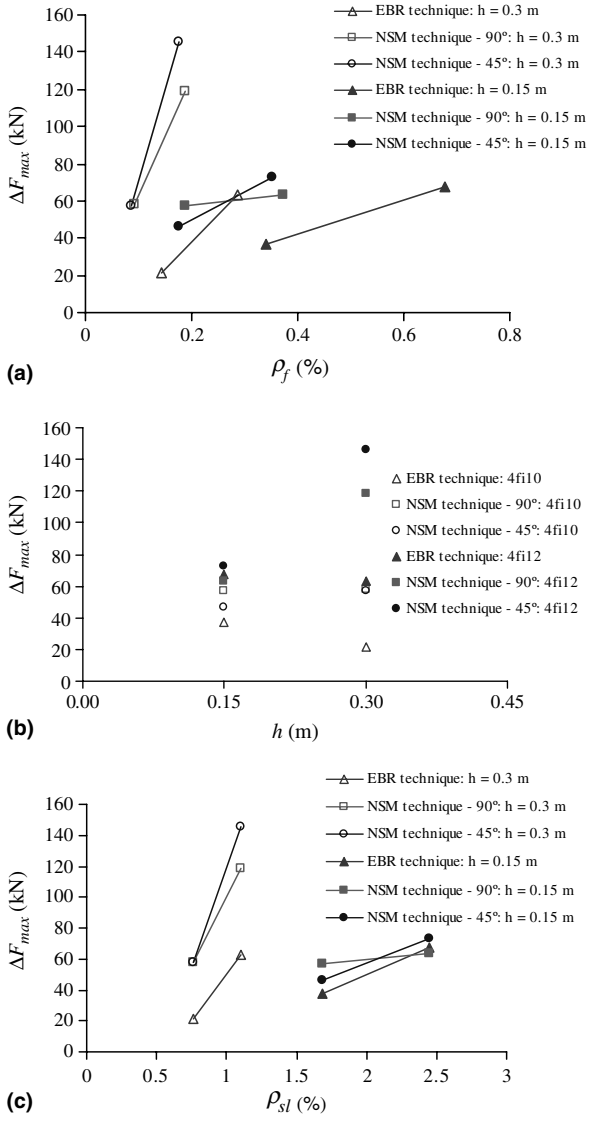

Fig. 13. Influence of the: (a) CFRP shear reinforcement ratio, (b) beam depth, (c) longitudinal steel reinforcement ratio, on the efficacy of the shear strengthening technique.

trend with $L_{tot\,min}$, and the maximum $L_{tot\,min}$ corresponds to A12_IL beam (see, for a while, Fig. 20).

Fig. 13c reveals that ΔF_{max} increased with ρ_{sl} and this increase was more pronounced in the highest beams strengthened by the NSM technique.

3.7. Profitability of the NSM technique

To assess the influence of the CFRP laminate orientation, not only in terms of increasing the beam load carrying capacity (F_{max}), but also in terms of the amount of consumed CFRP, the ratio $\Delta F_{max}/l_{CFRP}$ of the beams strengthened by the NSM technique was evaluated (designated profitability index), where ΔF_{max} is the increase in the F_{max} and l_{CFRP} is the total length of the laminates applied in the beam. The values included in Table 4 show that (see also Fig. 14), independent of the beam height and the

Table 4
Profitability index of the NSM technique

Series		Beam designation	F_{max} (kN)	ΔF_{max} (kN)	l_{CFRP} (m)	$\Delta F_{max}/l_{CFRP}$ (kN/m)
A ($h = 0.30$ m)	(4ϕ10)	A10_C	100.40	–	–	–
		A10_VL	158.64	58.24	4.80	12.13
		A10_IL	157.90	57.50	3.68	15.63
	(4ϕ12)	A12_C	116.50	–	–	–
		A12_VL	235.11	118.61	8.40	14.12
		A12_IL	262.38	145.88	7.35	19.85
B ($h = 0.15$ m)	(4ϕ10)	B10_C	74.02	–	–	–
		B10_VL	131.22	57.20	2.40	23.83
		B10_IL	120.44	46.42	1.97	23.56
	(4ϕ12)	B12_C	75.70	–	–	–
		B12_VL	139.20	63.50	4.20	15.12
		B12_IL	148.50	72.80	3.91	18.62

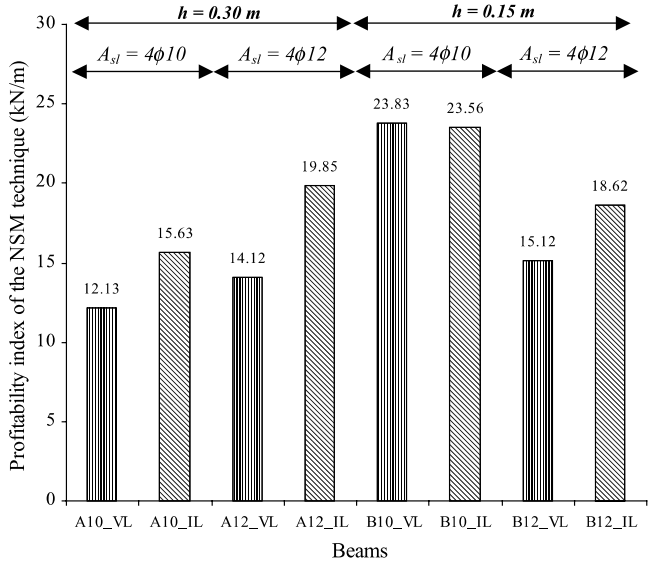

Fig. 14. Representation of the profitability index for the NSM technique.

longitudinal steel reinforcement ratio (ρ_{sl}), the profitability index was larger in the beams with laminates at 45°. For both the A series, the profitability index increased with the increase of ρ_{sl}. This tendency was not observed in both B series since the reduced bonded lengths of the CFRP laminates in these shallow beams limited the increase on the ΔF_{max}.

4. Appraisal the performance of analytical formulations

Taking the results obtained in the tested beams strengthened with EBR technique, the performance of the analytical formulations proposed by *ACI* [14] and *fib* [15] was appraised. The documents published by these institutions are not yet dealing with the NSM technique. Thereby, the applicability of the analytical formulation proposed by Nanni et al. [16] was checked, using for this purpose the experimental results obtained in the beams strengthened with NSM laminates. New estimates for the parameters of the model by Nanni et al. are proposed in order to take into account the bond stress and the CFRP effective strain values recorded in pullout bending tests [12].

4.1. ACI recommendations for EBR technique

According to *ACI* [14], the design value of the contribution of the FRP shear reinforcement is given by

$$V_{fd} = \phi\psi_f \frac{A_{fv} f_{fe} d_f}{s_f} \quad (1)$$

where ϕ is the strength-reduction factor required by *ACI* [23] that, for shear strengthening of concrete elements, has a value of 0.85, ψ_f is an additional reduction factor of 0.85 for the case of three-sided U-wraps (see Fig. 15), s_f is the spacing of the wet lay-up strips of FRP sheets, A_{fv} is the area of FRP shear reinforcement within spacing s_f,

$$A_{fv} = 2nt_f w_f \quad (2)$$

with n, t_f and w_f being the number of layers per strip, the thickness of a layer and the width of the strips. The effective stress in the FRP, f_{fe}, is obtained multiplying Young's modulus of the FRP, E_f, by the effective strain,

$$\varepsilon_{fe} = k_v \varepsilon_{fu} \leqslant 0.004 \quad \text{(for U-wraps)} \quad (3)$$

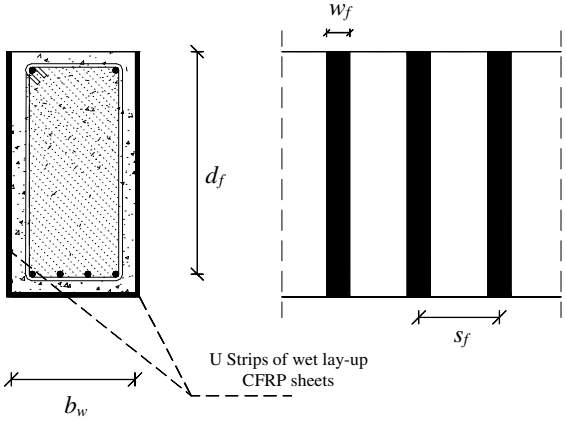

Fig. 15. Data for the externally bonded shear strengthening technique.

where k_v is a bond-reduction coefficient that is a function of the concrete strength, the type of wrapping scheme used, and the stiffness of the FRP,

$$k_v = \frac{k_1 k_2 L_e}{11900\varepsilon_{fu}} \leqslant 0.75 \quad (4)$$

with

$$L_e = \frac{23300}{(nt_f E_f)^{0.58}} \quad (5)$$

$$k_1 = \left(\frac{f'_c}{27}\right)^{2/3} \quad (6)$$

$$k_2 = \frac{d_f - L_e}{d_f} \quad \text{(for U-wraps)} \quad (7)$$

In (1) and (7) d_f is the effective depth of FRP shear reinforcement (see Fig. 15), and f'_c is the characteristic value of the concrete compressive strength [23]. The length and the force units of the variables in (4)–(7) are millimeter and Newton, respectively.

In Table 5, the values obtained with this formulation are compared to those registered experimentally. Apart beam B10_M, the *ACI* formulation has estimated a FRP contribution for the shear strengthening that was larger than the contribution recorded experimentally. A deficient bond of the strip crossed by the shear failure crack might have caused the high abnormal value of V_{fd}^{ana}/V_f^{exp} of A10_M beam, since this strip debonded prematurely (see Fig. 8).

4.2. *fib* recommendations for EBR technique

According to *fib* recommendations [15], the contribution of wet lay-up strips of FRP sheets for shear strengthening is evaluated by the following expression:

$$V_{fd} = 0.9\varepsilon_{fe,d} E_f \rho_f b_w d \quad (8)$$

where b_w and d are the width of the beam cross section and the distance from extreme compression fiber to the centroid of the nonprestressed steel tension reinforcement. In (8) ρ_f is the FRP shear reinforcement ratio,

$$\rho_f = \frac{A_{fv}}{b_w s_f} \quad (9)$$

and $\varepsilon_{fe,d}$ is the design effective strain in the FRP, that can be obtained from ε_{fe},

$$\varepsilon_{fe} = \min\left[0.65\left(\frac{f_{cm}^{2/3}}{E_f\rho_f}\right)^{0.56} \times 10^{-3}; 0.17\left(\frac{f_{cm}^{2/3}}{E_f\rho_f}\right)^{0.30}\varepsilon_{fu}\right] \quad (f_{cm} \text{ in MPa and } E_f \text{ in GPa}) \quad (10)$$

applying two safety factors, $\varepsilon_{fe,d} = 0.8\varepsilon_{fe}/1.3$, the first one, 0.8, to convert ε_{fe} in a characteristic value and the second one, 1.3, that depends on the FRP failure mode (in the present case, the beams strengthened by EBR technique failed by debonding). In (10) f_{cm} is the cylinder average concrete compressive strength and ε_{fu} is the ultimate FRP strain. The analytical and the experimental results are compared in Table 5. Apart beam B12_M, *fib* formulation has also predicted an FRP contribution larger than the experimentally registered values. Like in the *ACI* formulation, an abnormal high V_{fd}^{ana}/V_f^{exp} value was also obtained in A10_M beam, which stresses the suspicion that the strip crossing the shear failure crack was deficiently bonded.

Fig. 16 compares the values of the CFRP contribution for the shear strengthening according to *ACI* and *fib* formulations. In general, all the formulations estimated larger values than those registered experimentally. Apart B12_M beam, in the remaining beams the *ACI* formulation estimated lower values than *fib*.

Using similar EBR shear strengthening configuration, other researchers have obtained larger safety factors. However, these researchers have used wet lay-up CFRP sheets of Young's modulus (E_f) of about 220 GPa, and, in the major cases, the shear CFRP strips were formed of one layer. In the present research a CFRP sheet of $E_f = 390$ GPa and strips of two layers were used. This indicates that the expressions of ACI and *fib* formulations

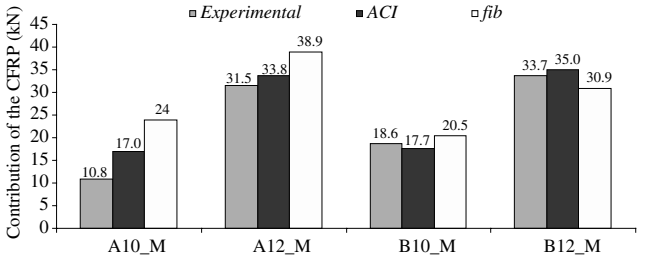

Fig. 16. Analytical vs experimental results (ACI and *fib* analytical formulation).

Table 5
Analytical vs experimental results (*ACI* and *fib* analytical formulations)

Beam designation	Experimental	ACI [a] formulation		*fib* [b] formulation		V_f^{exp}/V_{fd}^{ana} (ACI formulation)	V_f^{exp}/V_{fd}^{ana} (*fib* formulation)
	V_f^{exp} (kN)	ε_{fe} (‰)	V_{fd}^{ana} (kN)	ε_{fe} (‰)	V_{fd}^{ana} (kN)		
A10_M	10.8	2.50	17.0	4.62	24.0	0.64	0.45
A12_M	31.5	2.50	33.8	3.75	38.9	0.93	0.81
B10_M	18.6	2.42	17.7	3.66	20.5	1.05	0.91
B12_M	33.7	2.42	35.0	2.79	30.9	0.96	1.09

[a] f'_c values were obtained at the age of the beam tests ($f'_c = 40.2$ MPa for A series and $f'_c = 46.5$ MPa for B series).
[b] f_{cm} values were obtained at the age of the tested beams.

defining the FRP effective strain were not well calibrated for this situation, since they provide too high effective strain values when using stiffer shear CFRP systems. Therefore, more research is needed in this field.

4.3. Formulation by Nanni et al. for NSM technique

According to the formulation by Nanni et al. [16], the contribution of the NSM FRP elements for the shear strengthening is obtained from expression,

$$V_f = 4 \cdot (a_f + b_f) \cdot \tau_b \cdot L_{tot\,min} \tag{11}$$

where a_f and b_f are the dimensions of the laminate cross section, τ_b represents the average bond stress of the FRP elements intercepted by the shear failure crack, and $L_{tot\,min}$ is obtained from (see Fig. 17),

$$L_{tot\,min} = \sum_i L_i \tag{12}$$

where L_i represents the length of each single NSM laminate intercepted by a 45-degree shear crack expressed as

$$L_i = \begin{cases} \min\left(\frac{s_f}{\cos\alpha + \mathrm{sen}\alpha} i; l_{max}\right) & i = 1 \ldots \frac{N}{2} \\ \min\left(l_{net} - \frac{s_f}{\cos\alpha + \mathrm{sen}\alpha} i; l_{max}\right) & i = \frac{N}{2} + 1 \ldots N \end{cases} \tag{13}$$

$L_{tot\,min}$ corresponds to an arrangement of the FRP reinforcements crossing the shear failure crack that leads to the minimum of the $\sum_i L_i$. In (13) α represents the slope of the FRP laminate with respect to the beam longitudinal axis and l_{net} is defined as

$$l_{net} = l_b - \frac{2c}{\sin\alpha} \tag{14}$$

which represents the net length of a FRP laminate, as shown in Fig. 17, to account for cracking of the concrete cover and installation tolerances. In (14), l_b is the actual length of a FRP laminate and c is the concrete clear cover.

The first limitation of (13) takes into account bond as the controlling failure mechanism, and represents the minimum effective length of a FRP laminate intercepted by a shear crack as a function of the term N:

$$N = \frac{l_{eff}(1 + \cot\alpha)}{s_f} \tag{15}$$

where N is rounded off to the lowest integer (e.g., $N = 5.7 \Rightarrow N = 5$), and l_{eff} represents the vertical length of l_{net} as shown in Fig. 17 written as follows:

$$l_{eff} = l_b \sin\alpha - 2c \tag{16}$$

The second limitation in (13), $L_i = l_{max}$, results from the force equilibrium condition, taking an upper bound value for the effective strain, ε_{fe} (see Fig. 18),

$$l_{max} = \frac{\varepsilon_{fe}}{2} \cdot \frac{a_f \cdot b_f}{a_f + b_f} \cdot \frac{E_f}{\tau_b} \tag{17}$$

Adopting for ε_{fe} and τ_b the values recommended by Nanni et al. [16], 4‰ and 6.9 MPa, respectively, and assuming for Young's modulus of the laminate the average value recorded in the experimental program of the present work (166 GPa), the values of the contribution of the NSM laminates for the shear strengthening of concrete beams, included in Table 6, are compared to those registered experimentally (for ϕ and ψ_f a value of 0.85 was considered, following the recommendations of ACI [14]). This table does not include the data of the B10_VL beam since, according to the formulation by Nanni et al., the FRP contribution is null. An average V_f^{exp}/V_{fd}^{ana} ratio of about 2.51 was obtained, which is significantly larger than the value determined by Nanni et al. [16], which indicates that for τ_b and/or ε_{fe} too conservative values were adopted.

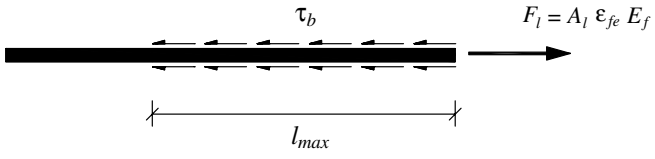

Fig. 18. Graphical representation of l_{max}.

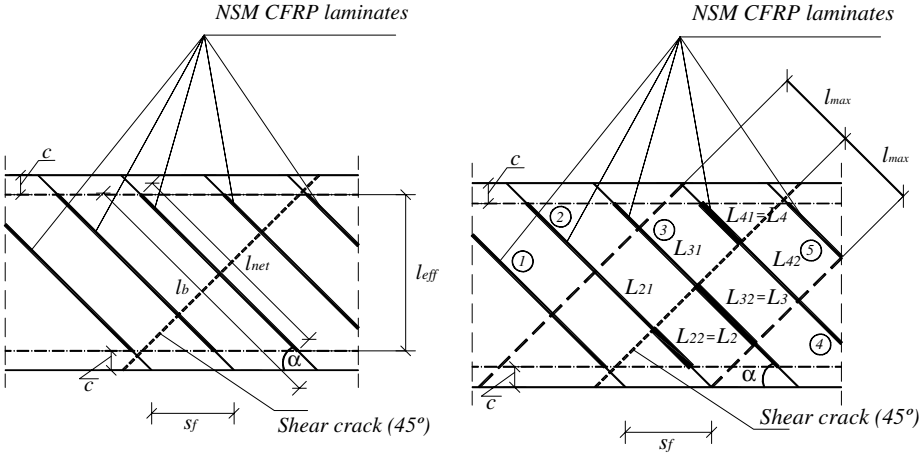

Fig. 17. Graphical representation of variables used in the formulation by Nanni et al. (for this example $\sum_i L_i = L_2 + L_3 + L_4$).

Table 6
Analytical vs experimental results for NSM technique

Beam designation	Experimental	Formulation by Nanni et al. [16]			
		$\varepsilon_f = 4.0‰$, $\tau_b = 6.9$ MPa and $E_f = 166$ GPa		$\varepsilon_f = 5.9‰$, $\tau_b = 16.1$ MPa and $E_f = 166$ GPa	
	V_f^{exp} (kN)	V_{fd}^{ana} (kN)	V_f^{exp}/V_{fd}^{ana}	V_{fd}^{ana} (kN)	V_f^{exp}/V_{fd}^{ana}
A10_VL	29.1	10.9	2.67	19.8	1.47
A10_IL	28.8	13.4	2.15	19.8	1.45
A12_VL	59.3	23.9	2.48	39.6	1.50
A12_IL	72.9	33.6	2.17	55.4	1.32
B10_IL	23.2	7.4	3.14	17.3	1.34
B12_VL	31.8	10.5	3.03	19.8	1.61
B12_IL	36.4	18.8	1.94	35.6	1.02

Since the value of 6.9 MPa for the τ_b was obtained from bond tests with round cross sectional FRP bars, pullout-bending tests [12], schematically represented in Fig. 19, were carried out to assess the average bond stress for the used rectangular cross sectional CFRP laminates. The specimen was composed of two blocks: block B where the CFRP was fixed to concrete along a bonded length of 325 mm; block A where the CFRP was bonded to concrete using distinct bond lengths (test region). This configuration assured that the bond failure would occur in block A. The slit where the CFRP was inserted had a 15 mm depth and a 3.3 mm width. The displacement transducer LVDT2 was used to control the test, at 5 μm/s, and to measure the slip at the loaded end, u_l, while LVDT1 recorded the slip at the free end, u_f. The strain gauge glued to the CFRP at the symmetry axis of the specimen was used to estimate the pullout force on the CFRP at the loaded end. The applied forces were measured using two load cells (LC1 and LC2) placed at the supports of the specimen. Bond lengths, L_b, of 40, 60 and 80 mm were considered for assessing its influence on bond behavior.

From the obtained peak pullout forces a τ_b of 16.1 MPa was determined, which is much larger than the value obtained by De Lorenzis [7] for the NSM FRP rod strengthening system ($\tau_b = 6.9$ MPa), and recommended by Nanni et al. [16]. This difference can be justified by the fact that in the present work the adhesive system in the slit is composed by two thin layers of quasi constant thickness, while in the groove of De Lorenzis bond tests [7] the adhesive material had a variable thickness, in consequence of the rectangular geometry of the groove and the circular geometry of the rod cross section.

The CFRP average strain (ε_f) in the bond length of the carried out pullout bending tests [12] was evaluated from the u_l and u_f slips. At peak pullout force, the ε_f of the series of L_b equal to 40, 60 and 80 mm was 4.2‰, 5.7‰ and 7.9‰, respectively, giving an average strain of 5.9‰.

Assuming that τ_b, ε_f and E_f are equal to 16.1 MPa, 5.9‰ and 166 GPa, respectively, the analytical results indicated in Table 6 were obtained. If the experimental results (V_f^{exp}) are compared to the analytical ones (V_{fd}^{ana}), an average V_f^{exp}/V_{fd}^{ana} ratio of about 1.39 was obtained. Since a safety factor of 1.79 ($V_c^{exp}/V_{cd}^{ana} = 1.79$) was obtained in the beams without any shear reinforcement (see Table 7), and a safety factor of 1.24 ($V_w^{exp}/V_{wd}^{ana} = 1.24$) was determined for the contribution of the steel stirrups for the shear resistance, the safety factor of 1.39 indicates that the formulation by Nanni et al. can be considered for the evaluation of the NSM CFRP laminates in the shear strengthening of concrete beams.

Expression (11) indicates that V_f is proportional to $L_{tot\,min}$. To check this assumption, Fig. 20 represents the relationship between the ΔF_{max} (equal to two times the contribution of the CFRP systems for the beam shear resistance, V_f) obtained experimentally in the beams strengthened by NSM technique and the $L_{tot\,min}$. From this figure

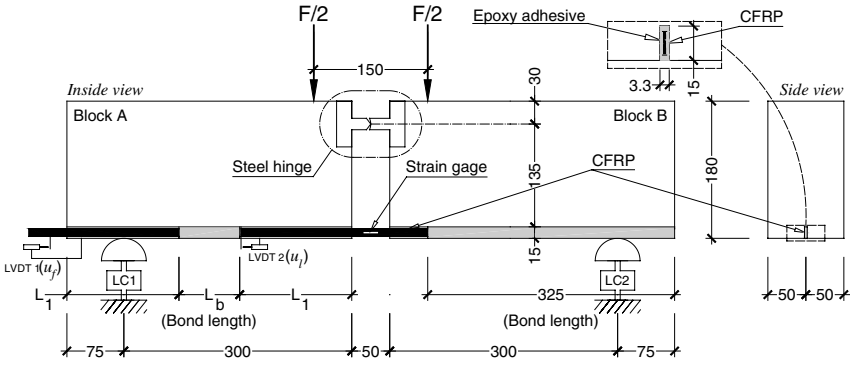

Fig. 19. Specimen of the pullout-bending tests.

Table 7
Analytical vs experimental results of the contribution of the concrete and steel stirrups for the shear resistance

Beam designation	Experimental		Analytical (Portuguese Code)		V_c^{exp}/V_{cd}^{ana}	V_w^{exp}/V_{wd}^{ana}
	V_c^{exp} (kN)	V_w^{exp} (kN)	V_{cd}^{ana} [a] (kN)	V_{wd}^{ana} [b] (kN)		
A10_C	50.2	–	34.9	–	1.44	–
A12_C	58.3	–	34.8	–	1.68	–
B10_C	37.0	–	18.6	–	1.99	–
B12_C	37.9	–	18.5	–	2.05	–
A10_S	50.2[c]	34.5	–	21.8	–	1.58
A12_S	58.3[c]	49.2	–	43.5	–	1.13
B10_S	37.0[c]	23.3	–	19.7	–	1.18
B12_S	37.9[c]	41.7	–	39.2	–	1.06

[a] $V_{cd}^{ana} = \tau_1 b_w d$.
[b] $V_{wd}^{ana} = 0.9d\frac{A_{sw}}{s}f_{syd}$.
[c] Values that were obtained in the reference beams.

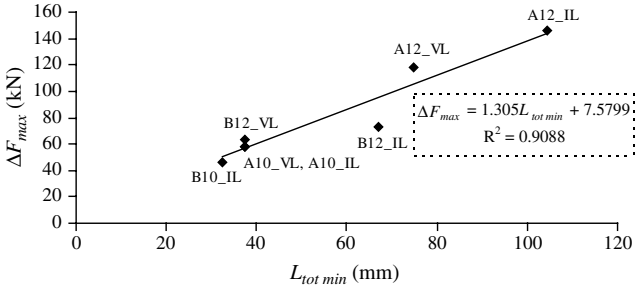

Fig. 20. Relationship between the contribution of the NSM CFRP shear strengthening system ($\Delta F_{max} = 2V_f$) and the total effective length of this strengthening system ($L_{tot\,min}$).

a clear linear increase trend between these two parameters is observed, which validates the aforementioned assumption.

5. Conclusions

To assess the effectiveness of near surface mounted (NSM) technique for the shear strengthening of concrete beams, four beam series of distinct depth and longitudinal tensile steel reinforcement ratio were tested under four point loads. Each series was composed of one beam without any shear reinforcement and one beam using the following shear reinforcing systems: conventional steel stirrups; strips of wet lay-up CFRP sheet embracing the bottom (in tension) and the lateral beam faces, designated by externally bonded reinforcing (EBR) technique; and laminates of CFRP embedded into vertical or inclined (45°) pre-cut slits on the concrete cover of the beam lateral faces (NSM strengthening technique). From the results obtained, the following main conclusions can be pointed out:

- The load carrying capacity of reinforced concrete beams failing in shear can be significantly increased using the CFRP shear strengthening systems applied in the present work.
- The NSM shear strengthening technique was the most effective of the CFRP systems. This efficacy was not only in terms of the beam load carrying capacity, but also in terms of deformation capacity at beam failure. Using the load carrying capacity, F_{max}, of the unreinforced beams, for comparison purposes, the beams strengthened by EBR and NSM techniques showed an average increase of 54% and 83%, respectively. The same comparison for the deflection at $0.95F_{max}$ after peak load (designated by deformability index, δ_p), showed that the increments were 77% and 307%, respectively, indicating that the efficacy of the NSM was more pronounced in terms of deformability index.
- In terms of F_{max} and δ_p of the beams reinforced with steel stirrups, the NSM strengthening technique provided almost similar F_{max} and an increase of 9% in the δ_p.
- Failure modes of the beams strengthened by the NSM technique were not as brittle as the ones observed in the beams strengthened by the EBR technique.
- The NSM shear strengthening technique was easier and faster to apply than the EBR technique.
- The design values of the contribution of the CFRP EBR strengthening systems for the beam shear resistance, evaluated from the *ACI* and *fib* formulations were 2% and 8% higher than the values registered experimentally, respectively.
- Assuming a bond stress of 16.1 MPa and an effective strain of 5.9‰ (average values of the data recorded in pullout bending tests), the formulation by Nanni et al. for the NSM technique predicted a CFRP contribution around 72% of the experimentally registered values, which indicates to be a formulation that can be considered for the design of the contribution of the CFRP NSM shear strengthening system.

Acknowledgements

The authors wish to acknowledge the supports provided by the S&P®, BeTTor MBT® Portugal, Secil (Unibetão), and the collaboration of Cemacom. The study reported

in this paper forms a part of the research program "CUTINSHEAR—Performance assessment of an innovative structural FRP strengthening technique using an integrated system based on optical fiber sensors" supported by FCT, POCTI/ECM/59033/2004.

References

[1] Taerwe L, Khalil H, Matthys S. Behaviour of RC beams strengthened in shear by external CFRP sheets. In: Proceedings of the third international symposium non-metallic (FRP) reinforcement for concrete structures, vol. 1, Tokyo, October, 1997. p. 483–90.

[2] Chaallal O, Nollet MJ, Perraton D. Shear strengthening of RC beams by externally bonded side CFRP strips. J Compos Construct 1998;2(2):111–3.

[3] Triantafillou T. Shear strengthening of reinforced concrete beams using epoxy-bonded FRP composites. ACI Struct J 1998(March–April): 107–115.

[4] Khalifa A, Gold WJ, Nanni A, Aziz MIA. Contribution of externally bonded FRP to shear capacity of RC flexural members. J Compos Construct 1998;2(4):195–202.

[5] Triantafillou T, Antonopoulos CP. Design of concrete flexural members strengthened in shear with FRP. J Compos Construct 2000;4(4):198–205.

[6] Basler M, White D, Desroches M. Shear strengthening with bonded CFRP L-shaped plates. In: Sami Rizkalla, Antonio Nanni, editors. Field applications of FRP reinforcement: case studies. ACI International SP-215; 2003. p. 373–84.

[7] De Lorenzis L. Strengthening of RC structures with near-surface mounted FRP rods. PhD Thesis in Civil Engineering, Universita' Degli Studi di Lecce, Italy, May, 2002, 289 pp.

[8] De Lorenzis L, Nanni A. Characterization of FRP rods as near-surface mounted reinforcement. J Compos Construct 2001;5(2):114–21.

[9] De Lorenzis L, Rizzo A, La Tegola A. A modified pull-out test for bond of near-surface mounted FRP rods in concrete. Composites: Part B 2002(33):589–603.

[10] Barros JAO, Sena-Cruz JM, Dias SJE, Ferreira DRSM, Fortes AS. Near surface mounted CFRP-based technique for the strengthening of concrete structures. In: Workshop on R+D+I in technology of concrete structures—tribute to Dr. Ravindra Gettu, Barcelona, Spain, 2004. p. 205–17.

[11] Barros JAO, Fortes AS. Flexural strengthening of concrete beams with CFRP laminates bonded into slits. J Cement Concrete Compos 2005;27(4):471–80.

[12] Sena-Cruz JM, Barros JAO. Bond between near-surface mounted CFRP laminate strips and concrete in structural strengthening. J Compos Construct 2004;8(6):519–27.

[13] Sena-Cruz JM, Barros JAO. Modeling of bond between near-surface mounted CFRP laminate strips and concrete. Comput Struct J 2004;82/17–19:1513–21.

[14] ACI Committee 440. Guide for the design and construction of externally bonded FRP systems for strengthening concrete structures. American Concrete Institute, ACI Committee 440, 2002, 118 pp.

[15] fib—Bulletin 14. Externally bonded FRP reinforcement for RC structures. Technical report by Task Group 9.3 FRP (Fiber Reinforced Polymer) reinforcement for concrete structures, Féderation Internationale du Béton—fib, July, 2001, 130 pp.

[16] Nanni A, Di Ludovico M, Parretti R. Shear strengthening of a PC bridge girder with NSM CFRP rectangular bars. Adv Struct Eng 2004;7(4):97–109.

[17] CEB-FIP Model Code. Comite Euro-International du Beton, Bulletin d'Information n° 213/214, 1993.

[18] EN 10 002-1. Metallic materials. Tensile testing. Part 1: Method of test (at ambient temperature). 1990, 35 pp.

[19] ISO 527-5. Plastics—Determination of tensile properties—Part 5: Test conditions for unidirectional fibre-reinforced plastic composites. International Organization for Standardization, Genève, Switzerland, 1997, 9 pp.

[20] Barros JAO, Sena-Cruz JM. Fracture energy of steel fibre reinforced concrete. J Mech Compos Mater Struct 2001;8(1):29–45.

[21] Gopalaratnam VS et al. Fracture toughness of fiber reinforced concrete. ACI Mater J 1991;88(4):339–53.

[22] JSCE—The Japan Society of Civil Engineers. Part III—2 method of tests for steel fiber reinforced concrete. Concrete Library of JSCE, No. 3, 1984.

[23] ACI Committee 318. Building code requirements for structural concrete and commentary. American Concrete Institute, Reported by ACI Committee 118, 2002.